REGULAR ARTICLE

blood advances

BMX kinase mediates gilteritinib resistance in *FLT3*-mutated AML through microenvironmental factors

Daelynn R. Buelow,[1,*] Bhavana Bhatnagar,[2,*] Shelley J. Orwick,[1] Jae Yoon Jeon,[1] Eric D. Eisenmann,[1] Jack C. Stromatt,[1] Navjot Singh Pabla,[1] James S. Blachly,[3] Sharyn D. Baker,[1] and Bradley W. Blaser[3]

[1]Division of Pharmaceutics and Pharmacology, College of Pharmacy, Comprehensive Cancer Center, The Ohio State University, Columbus, OH; [2]West Virginia University Cancer Institute, Department of Hematology and Medical Oncology, Wheeling, WV; and [3]Division of Hematology, College of Medicine, The Ohio State University Comprehensive Cancer Center, Columbus, OH

Key Points

- Resistance to gilteritinib remains an issue.
- BMX and microenvironment-mediated factors play a role in gilteritinib resistance.

Despite the clinical benefit associated with gilteritinib in relapsed/refractory acute myeloid leukemia (AML), most patients eventually develop resistance through unknown mechanisms. To delineate the mechanistic basis of resistance to gilteritinib, we performed targeted sequencing and scRNASeq on primary *FLT3*-ITD-mutated AML samples. Co-occurring mutations in *RAS* pathway genes were the most common genetic abnormalities, and unresponsiveness to gilteritinib was associated with increased expression of bone marrow-derived hematopoietic cytokines and chemokines. In particular, we found elevated expression of the TEK-family kinase, BMX, in gilteritinib-unresponsive patients pre- and post-treatment. BMX contributed to gilteritinib resistance in *FLT3*-mutant cell lines in a hypoxia-dependent manner by promoting pSTAT5 signaling, and these phenotypes could be reversed with pharmacological inhibition and genetic knockout. We also observed that inhibition of BMX in primary *FLT3*-mutated AML samples decreased chemokine secretion and enhanced the activity of gilteritinib. Collectively, these findings indicate a crucial role for microenvironment-mediated factors modulated by BMX in the escape from targeted therapy and have implications for the development of novel therapeutic interventions to restore sensitivity to gilteritinib.

Introduction

Acute myeloid leukemia (AML) is characterized by the atypical proliferation of immature myeloblasts, ultimately affecting normal hematopoiesis. Activating internal tandem duplication (ITD) mutations within *FLT3* (Fms-like tyrosine kinase 3) are a common mutation found in AML.[1-3] Individuals with *FLT3*-ITD mutations have a higher rate of relapse and poor prognosis.[4-7] *FLT3*-ITD mutations have been and still are an attractive candidate for targeted tyrosine kinase inhibitors given their pathobiological and prognostic role in AML. A number of first- and second-generation FLT3 inhibitors have been evaluated at preclinical and clinical trial levels. To date, two FLT3 inhibitors, midostaurin and gilteritinib, have been approved by the FDA.[8,9] Gilteritinib received FDA approval in the treatment of relapsed/refractory AML with *FLT3* mutations (*FLT3*+), based on promising data in the ADMIRAL trial demonstrating longer survival and

Submitted 26 April 2022; accepted 27 June 2022; prepublished online on *Blood Advances* First Edition 7 July 2022; final version published online 31 August 2022. DOI 10.1182/bloodadvances.2022007952.

*D.R.B. and B.B. contributed equally to this study.

All analysis scripts are available at https://github.com/blaserlab/flt3_aml_bakerlab. A companion pre-processed R data package is available at https://datadryad.org/stash/share/RiU-HT6E5zL0wNVkjocVwJzxAYWmKwsakg8Kze5Z68k (https://doi.org/10.5061/dryad.zgmsbccdc). Raw sequencing data has been deposited at Gene Expression Omnibus (accession number GSE199333).

The full-text version of this article contains a data supplement.

higher rates of remission with gilteritinib compared with untargeted salvage chemotherapy.[9] Even though gilteritinib is effective in the setting of relapsed/refractory *FLT3*+ AML, lack of response or relapse after initial response due to intrinsic or adaptive resistance mechanisms are inevitable consequences of the disease in the absence of hematopoietic stem cell transplantation.[10] A limited number of studies have looked at mechanisms of gilteritinib resistance. DNA sequencing and in vitro validation revealed that during gilteritinib treatment, the acquisition of RAS pathway mutations within individual *FLT3*+ cells leads to changes in clonal architecture and resistance to therapy.[11] Other in vitro and in vivo studies utilizing *FLT3*+ cell lines suggested metabolic reprogramming as a possible resistance mechanism.[12,13] It was observed that initial gilteritinib-resistance in cell lines involved a unique metabolic profile with alterations in sphingolipid metabolism, as well as carnitine/fatty acid metabolism.[12] Furthermore, analysis of xenograft models at disease progression after gilteritinib treatment revealed distinct adaptations in glutamine uptake, utilization, and metabolism leading to cellular senescence.[13]

To identify novel mechanisms of gilteritinib resistance, we used single-cell RNA sequencing (scRNASeq) on primary patient samples collected during gilteritinib treatment. In unresponsive patients, we observed upregulation of bone marrow (BM)-derived cytokines and chemokines as well as BMX, a nonreceptor kinase belonging to the TEC family of kinases. In both ex vivo and in vitro experiments under conditions mimicking the tumor microenvironment, we show that BMX contributed to gilteritinib resistance, which was reversed with pharmacological inhibition and genetic knockout (KO). We demonstrate that BMX inhibition modulated the cytokine/chemokine network and enhanced the activity of gilteritinib, thereby linking BMX and microenvironmental factors in resistance. Taken together, our analysis implicates microenvironment-dependent escape from targeted therapy as a means of clinical drug resistance and provides a deeper understating of the targets and pathways that play important roles in response to gilteritinib treatment.

Methods

Patients and samples

Samples were obtained from 19 *FLT3*+ AML patients receiving gilteritinib on the Expanded Access Trial (NCT03070093) or standard of care after November 2018. Patient characteristics and prior therapy at time of study entry are listed in Table 1 and supplemental Table 1. Changes in hematologic parameters, myeloblast counts during treatment, and response are listed in supplemental Table 2. BM and peripheral blood samples were enriched for leukemic myeloblasts by ficoll purification and viably frozen in the OSUCCC Leukemia Tissue Bank Shared Resource (LTBSR). In some cases, BM cells were fixed in 3:1 mixture of methanol and glacial acetic acid. All treatments and clinical monitoring were approved by the Institutional Review Board (IRB), and informed consent was obtained from all patients. Samples were obtained on IRB-approved protocol OSU-1997C0194 and sample and data analysis was performed under IRB-approved protocol OSU-19093.

Targeted gene sequencing

Targeted sequencing for mutational status was carried out on 80 coding genes.[14] A variant allele fraction (VAF) cutoff of 0.05 was set for reporting mutations. If a VAF of 0.05 was observed, visual inspection of samples taken before and after the given time point were analyzed for the mutation. If the mutation was observed and Q-score was $\geq$27, the mutation was included in our analysis. Single nucleotide polymorphisms with no known pathogenic association were not reported as mutations. Visual inspection of all variants was carried out using Integrative Genomics Viewer v.2.8 (Broad Institute).

scRNASeq

scRNASeq was carried out on viable frozen Ficoll-enriched myeloblast samples from eight matched patient samples before and during gilteritinib treatment. Cells were thawed, washed with PBS, and dead cells were removed using a Dead Cell Removal Kit (Miltenyi). Cells were then washed twice using scRNASeq Buffer (PBS + 0.04% BSA) to remove any Ca^{2+} and resuspended at a concentration of 1×10^6/mL. Approximately 6000 cells per lane were loaded and processed for cDNA according to the 10X Genomics Chromium Single Cell 3′ Reagent Kit v.3.1 in the OSUCCC Genomics Shared Resource. Samples with less than 10% myeloblasts, estimated by diagnostic pathology report, were run in duplicate or triplicate to obtain a minimum of approximately 400 myeloblast cells. Libraries were sequenced on the NovaSeq 6000 using 300 cycles with paired 150-bp reads. A minimum of 20 000 read pairs per cell were obtained.

FASTQs, BAM files, and cell barcode-gene matrices were generated with Cellranger v3.1.0 using the 10×-supplied GRCh38 reference (v.2020-A). QC functions from *scater*[15] were used to remove cells with a proportion of counts mapped to mitochondrial genes that was more than 2 median absolute deviations above the median, a feature count that was more than 2 median absolute deviations below the median or cells with more than 1% of counts mapped to a globin gene. High-likelihood doublets were predicted using *Doubletfinder*[16] and removed. Patient-to-patient variation was reduced by aligning according to mutual nearest neighbors with *Batchelor*.[17] Following alignment according to patient ID, a second round of alignment by sample tissue type (blood or BM) was performed. After QC, data were available from 20 samples from seven unique patients before and after treatment. Dimension reduction, clustering, top marker identification, gene module analysis, and quantification of gene expression was performed using functions from Monocle3.[18,19] Cell clustering was performed using the partitioning method.[20] Descriptive labels were attached to cell partitions by inspection of top specific markers (supplemental Table 3), aggregated gene module expression (supplemental Table 4), and by label transfer from reference PBMC and BM data sets using *Seurat*.[21] Pseudobulk differential gene expression was performed (supplemental Tables 5-6) by generating aggregate gene expression profiles for indicated strata of cells using Monocle3 functions and then comparing across conditions using *DESeq2*.[22] Each patient served as an independent biological replicate in this analysis.

Cell interactions were inferred using CellChat.[23] Briefly, the scRNA-seq dataset was stratified by individual patient and timepoint relative to gilteritinib administration (pre, post). Expression of cell-extracellular matrix, direct cell-cell, and soluble ligand-receptor pairs were calculated for the cell populations shown later in Figure 2A. A score was generated for all possible interactions; autocrine myeloblast-myeloblast interactions were selected and filtered to include only those with $P < .05$.

Table 1. Patient baseline characteristics and prior therapy

Variable	Number (%)
Gender, male	14 (72.7)
Age in years, median (range)	59 (29-76)
Disease status	
Relapsed	10 (52.6)
Refractory	8 (42.1)
Other*	1 (5.3)
ELN cytogenetic risk	
Favorable	1 (5.3)
Intermediate	17 (89.5)
Adverse	1 (5.3)
Peripheral WBC $\times 10^9$ cells/L, median (range)	4.8 (<0.3-79.1)
Peripheral myeloblast %, median (range)	17.5 (0-98)
Bone marrow myeloblast %, median (range)	52.5 (2-94)
FLT3 mutation status	
ITD positive	17 (89.5)
Both ITD and TKD positive	1 (4.5)
TKD positive	1 (4.5)
Bone marrow transplant	
Pre	11 (57.9)
Post	8 (42.1)
Prior therapy	
Newly diagnosed	
7 + 3	1 (5.3)
7 + 3 and/or HiDAC + midostaurin	14 (73.7)
BI 836858 + azacytidine	1 (5.3)
Entospletinib + azacytidine	1 (5.3)
Enasidenib	1 (5.3)
Unknown	1 (5.3)
Relapsed/refractory disease (before gilteritinib)	
Pacritinib, selinexor + mitoxantrone/etoposide/cytarabine, sorafenib	1 (5.3)
Venetoclax + azacytidine, AZD5991	1 (5.3)
FLAG + HMA	1 (5.3)

7 + 3, cytarabine continuously for 7 days with an anthracycline days 1 to 3; FLAG, fludarabine with HiDAC, idarubicin, and granulocyte-colony stimulating factor; HiDAC, high-dose cytarabine; HMA, hypomethylating agent.
*Gilteritinib treatment post-transplant.

Spectral flow cytometry

Ficoll-enriched BM cells were stained with LIVE/DEAD Blue (ThermoFisher), blocked with FC block (BD Biosciences) and stained with CD45-Amycan (clone: 2D1, BD Biosciences), CD33-BUV395 (clone: P67.6, BD Biosciences), and FLT3 (CD135)-BV421 (clone: 4G8, BD Biosciences). Cells were then fixed with BD Cytofix buffer (BS Biosciences) and permeabilized with BD phosflow perm buffer III (BD Biosciences). Cells were then stained with pSTAT5-PE (clone: 47/Stat5, BD Biosciences). Sample analysis was performed in the OSUCCC Flow Cytometry Shared Resource and Immune Monitoring & Discovery Platform using the Cytek Aurora. Data were analyzed using FCS Express v.7 (De Novo Software).

Cells and culturing conditions

MOLM-13 (DSMZ), and MV4-11 (DSMZ and ATCC) cells were maintained and grown in 10% FBS RPMI-1640 media under normoxic conditions, which was in a 37°C humidified incubator with 5% CO_2. For ex vivo testing, human primary AML samples were obtained from the LTBSR (under IRB-approved protocol OSU-1997C0194) and cultured in 10% FBS RPMI-1640 media supplemented with 10 ng/mL each of hSCF, hIL-3, hGM-CSF, and hFLT3 ligand (Peprotech), as well as 1× Anti-anti (ThermoFisher). For hypoxia growth, cells were shifted to a 37°C humidified glove box (COY labs) with 5% CO_2, 94% N_2, and 1% O_2 for a minimum of 24 hours. STR DNA profiling was carried out on all cell lines to confirm identification. Additionally, cell lines were routinely tested for mycoplasma contamination.

MV4-11 BMX CRISPR KO was conducted by Synthego (Menlo Park, CA). Briefly, sgRNA targeting exon 3 was used to engineer a KO cell line. Individual BMX CRISPR KO clones were isolated by limiting dilution. KO clones were verified by Sanger sequencing and western blots.

Cell viability assessment

Cells were plated (cell line: 0.15 × 10^6/mL, primary samples: 1 × 10^6/mL) and cultured in normoxia or hypoxia for 24 hours. Cells were then treated with gilteritinib (ChemiTek), BMX-IN-1 (Calbiochem), CHMFL-BMX-078 (Medchem Express), and remibrutinib (Medchem Express) alone or in combination for 48 hours under the respective conditions. Cell viability was then assessed by MTT (3-[4,5-Dimethyl-2-thiazolyl]-2,5-diphenyl-2H-tetrazolium bromide; Sigma Aldrich) assay for cell lines or CellTiter Glo (Promega) for primary samples. Growth curve on primary samples was carried out after growth in hypoxia for 24 hours and then treatment with DMSO, gilteritinib, CHMFL-BMX-078, or in combination for up to 72 hours. CellTiter Glo assay was performed at the indicated time points. Surface response method was assessed from the dose response curve for synergy, additivity, or antagonism between gilteritinib and CHMFL-BMX-078 using Combenefit software.[24] Experiments were carried out in either duplicate or triplicate with six replicates, with the exception of primary samples, which were carried out once with three replicates.

Cytokine/chemokine measurement

Cytokine/chemokine concentrations were measured in culture media collected from primary *FLT3*+ AML samples, or cell lines using a multiplexed MILLIPLEX MAP Human Cytokine/Chemokine magnetic bead kit (Millipore Sigma) for the CCL2-4/CXCL1/8 cluster and CCL5. Technical replicates were collected for primary AML samples and technical, as well as biological replicates were collected for cell lines. This assay was carried out according to manufacturer's details with an initial overnight incubation. Samples were analyzed using a MAGPIX analyzer (Luminex). A minimum of 50 beads per analyte was used to determine the raw mean fluorescent intensity (MFI). MILLIPLEX analyst software (Millipore Sigma) was used to calculate pg/mL from MFI, utilizing the standard curves included in the kit.

Results

Co-occurring mutation analysis

As we know, the mutational landscape plays an important role in treatment response, but also has the ability to evolve during treatment.

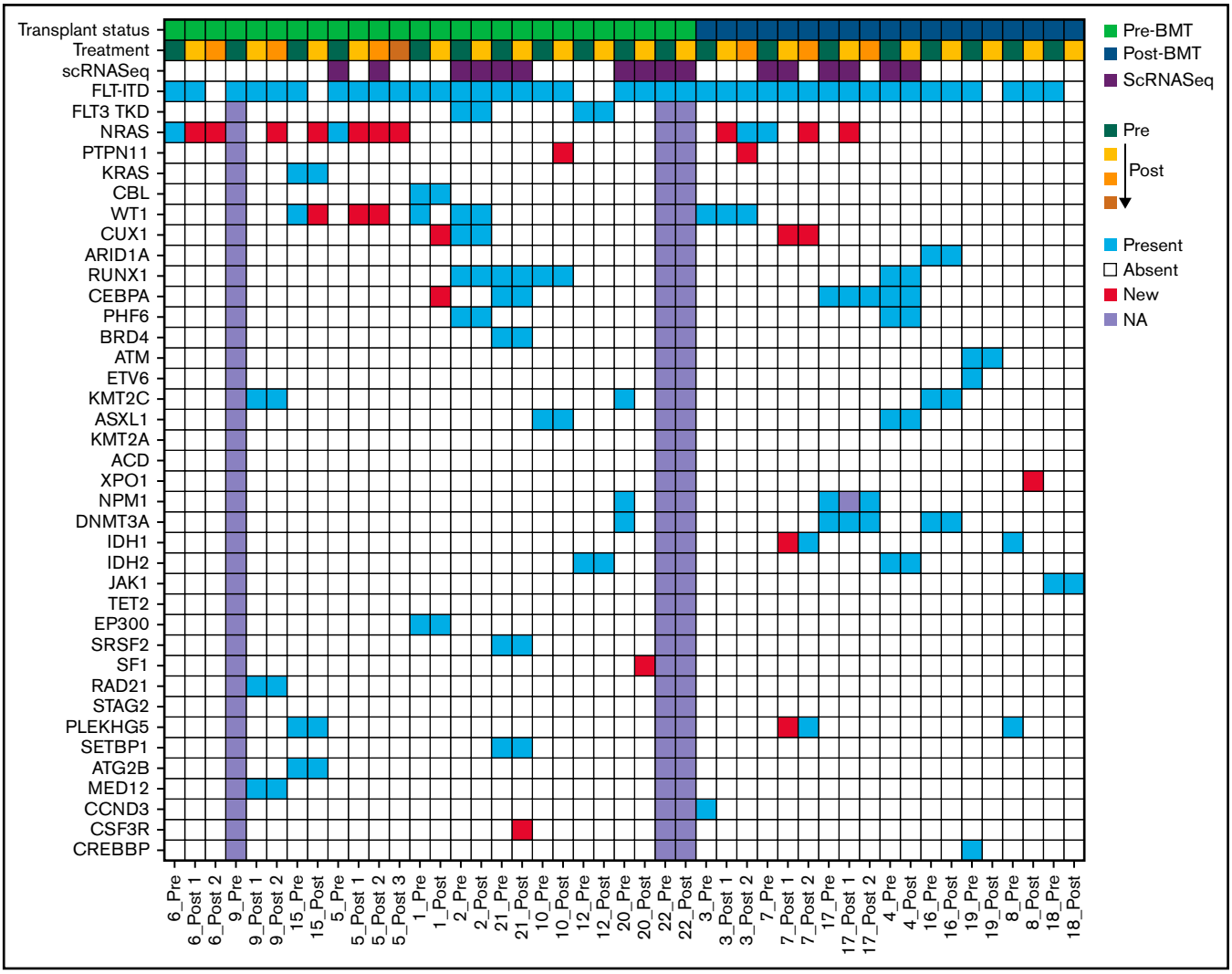

Figure 1. Oncoprint of mutations in gilteritinib treated patients pre- and post-treatment. Row 1 indicates the transplant status of the patient; relapsed/refractory pre-bone marrow transplant (BMT) or post-BMT. Row 2 shows progression of treatment with green indicating pre-treatment samples and yellow indicating post initiation with an increasing gradient showing progression of treatment. Row 3 displays scRNASeq samples. Row 4 designates the FLT3 status. The patient ID is indicated below each column. Each remaining row represents genes mutated with a variant allele frequency (VAF) cut-off of 0.05. Blue indicates present, red is new/emerging, white is absent and lavender is not available.

Thus, we used targeted gene sequencing to determine the co-occurring mutational landscape in primary AML samples obtained before and during gilteritinib treatment. Patients had a median of 3.5 co-occurring mutations (range 1-6 mutations) in addition to *FLT3*-ITD. In pre- and post-treatment samples, mutations were observed in 35 and 37 genes, respectively. Most mutations fell into gene classes associated with RAS pathway genes, tumor suppressors, epigenetic modifiers,, kinases, and transcription factors (Figure 1). Among the RAS pathway mutations, a total of eight patients presented with RAS mutation. Four patients contained RAS pathway mutations in pre-treatment samples. In these four patients, all patients acquired additional RAS pathway mutations post-treatment. We observed an additional four patients with new RAS pathway mutation presenting at post-treatment (Figure 1; supplemental Table 7). The emergence of RAS pathway mutations at progression post gilteritinib treatment have been reported previously.[11] Additionally, we observed pre-treatment mutations in *CSF3R*, and *PLEKHG5*, as well as new mutations post treatment in *CSF3R*, *PLEKHG5*, *CUX1*, and *XPO1*, which have not been previously identified in gilteritinib-treated patients (Figure 1; supplemental Figure 1). Although mutation VAF fluctuated during treatment, the mutational landscape was generally maintained over treatment regardless of clinical response, even in cases of low myeloblast counts and after BM transplant (supplemental Figure 1; supplemental Table 7).

scRNASeq profiling of gilteritinib-unresponsive AML samples reveal adaptive mechanisms of gilteritinib resistance

We used scRNASeq to analyze the transcriptional state of myeloblast populations seen in gilteritinib-sensitive and -unresponsive patients. Patients were considered gilteritinib sensitive if their myeloblast counts decreased by 50% or greater during the course of treatment (supplemental Table 2). Four responsive patients received front-line

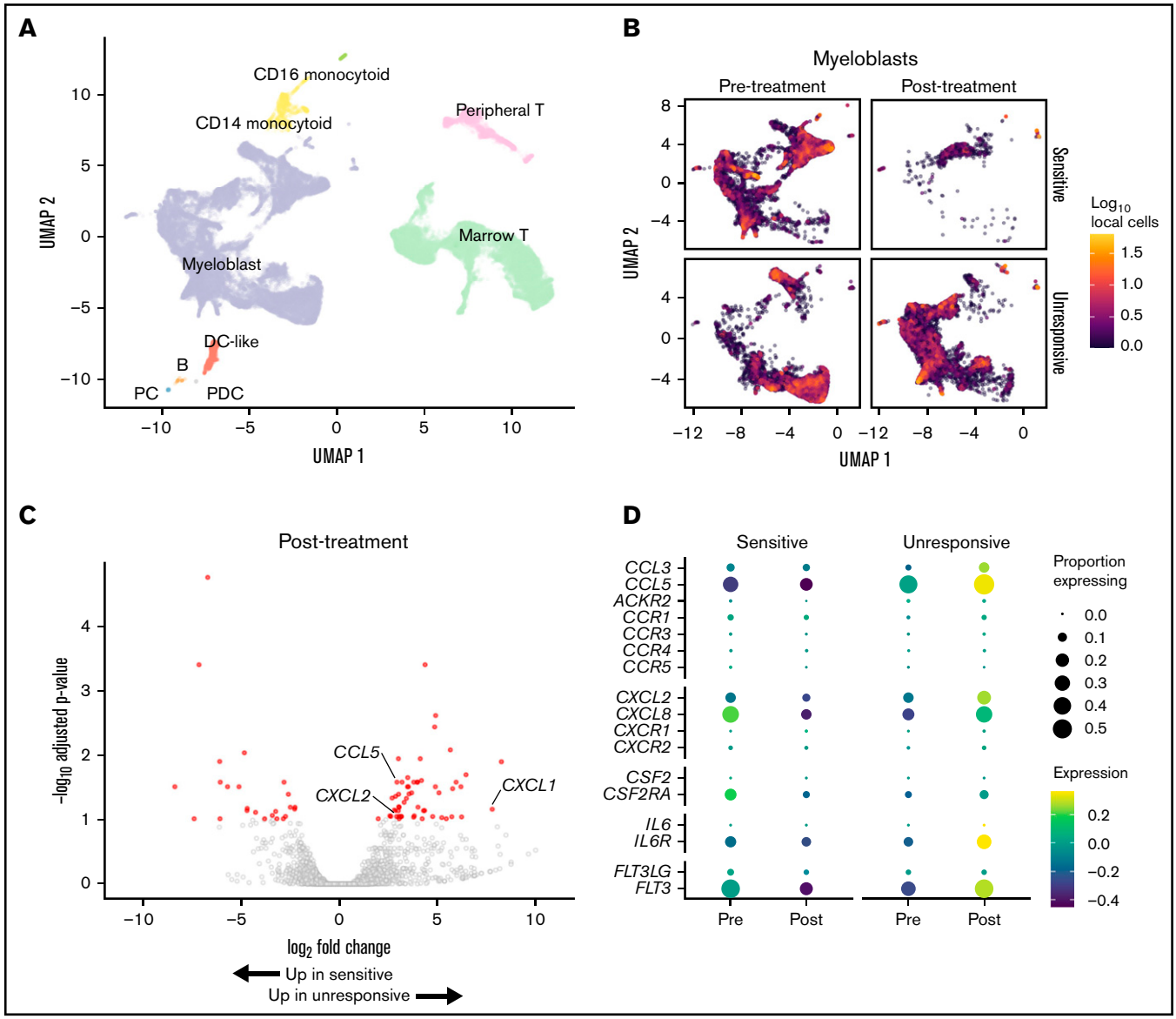

Figure 2. Single cell RNA-seq reveals gene expression alterations in response treatment. (A) UMAP representation of the complete dataset of 76 862 quality-filtered cells. (B) Myeloblast cells stratified by gilteritinib response (rows) and timepoint relative to starting therapy (columns). Cell color is calculated as the $\log_{10}$-transformed cell count within hexagonal bins. (C) Differential gene expression for gilteritinib-unresponsive patients. Red indicates genes with adjusted $P < .1$ and fold change ≥1.5; see also supplemental Table 6. (D) Expression of cytokine/chemokines and cytokine receptors pre-and post-treatment in gilteritinib-sensitive and -unresponsive patients. Circle size, fractional proportion of cells expressing a given marker; color scale, scaled expression level.

treatment with 7 + 3/midostaurin prior to gilteritinib. Of the three patients that were unresponsive to gilteritinib, one received treatment with 7 + 3/midostaurin before gilteritinib; one received 7 + 3/midostaurin followed by FLAG/HMA prior to gilteritinib; and one received BI 836858/azacytidine as frontline therapy followed by venetoclax/azacytine then AZD5991 before gilteritinib. High-quality data were acquired from 76 862 cells after QC. Cell clusters were generated by partitioning and cell identities were established by expression of canonical gene markers and label transfer from reference data sets (Figure 2A; supplemental Figure 2A-B; supplemental Table 3). Based on UMAP dimensionality reduction, there were clear differences in global transcriptional state within the myeloblast population between pre- and post-treatment samples and between gilteritinib-sensitive and -unresponsive patients (Figure 2B). After treatment was initiated, a significant decrease in the myeloblast population in the sensitive group was observed, as expected based on clinical myeloblast counts. The myeloblast population was maintained in the unresponsive group; however, there was a shift in the UMAP coordinates of this group, suggesting overall change in transcriptional state after initiating gilteritinib treatment (Figure 2B).

Given the differences we observed in the global transcriptional state of the myeloblast populations, we stratified the cells by treatment timepoint and used pseudobulk RNA-seq analysis to examine genes

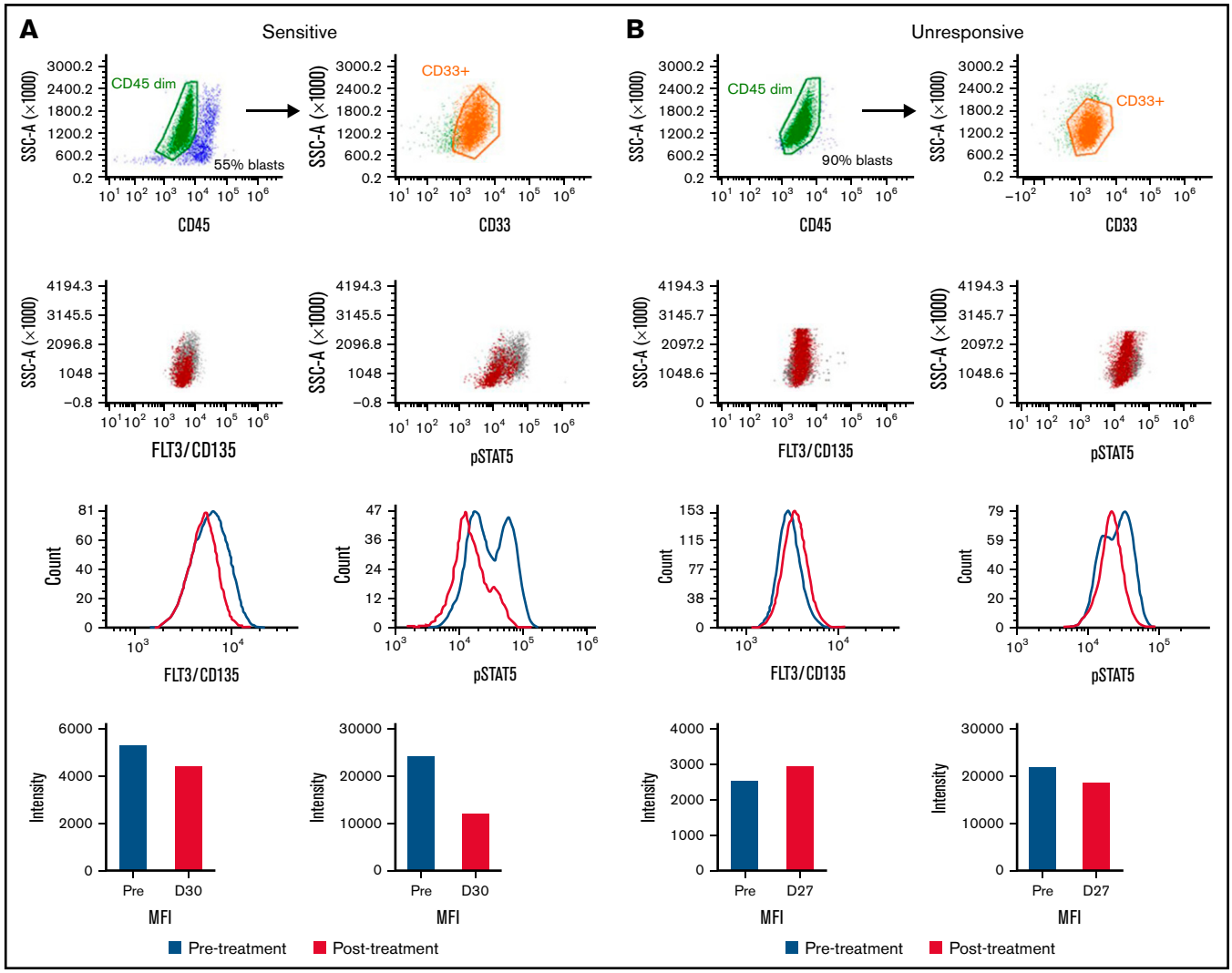

Figure 3. FLT3 and pSTAT5 expression in response to gilteritinib treatment. Using spectral flow, a sensitive (A) and an unresponsive (B) primary sample were first gated for myeloblasts using AML surface markers (CD45 dim and CD33^{+}) and then FLT3/CD135 and pSTAT5 expression. Pre-treatment samples are indicated in blue, and post-treatment samples are indicated with red. MFI, mean fluorescent intensity.

that were differentially regulated between gilteritinib-sensitive and -unresponsive patients post-treatment to identify potential mechanisms of adaptive resistance (Figure 2C; supplemental Table 6). Expression of cytokines and chemokines was upregulated in gilteritinib-unresponsive patients, including *CCL5*, *CXCL1*, and *CXCL2* (Log_2-fold change, 2.90, 7.76, and 3.00; adjusted *P* values, 0.0264, 0.069, and 0.089, respectively; Figure 2C; supplemental Table 6). The observation that *CXCL1* and *CXCL2* were upregulated along with *CCL5* is noteworthy given that resistance to FLT3 inhibitors due to BM-derived hematopoietic and inflammatory cytokines/chemokines has been documented in preclinical studies.[25-29] Based on these findings, exploratory analysis into expression of other cytokines, including CXCL8, showed a clear pattern of downregulation in gilteritinib-sensitive patients on treatment but upregulation in gilteritinib-unresponsive patients on treatment (Figure 2D). By contrast, expression of the receptors for these cytokines by myeloblasts was low (Figure 2D). Using the CellChat algorithm to infer cell interactions,[23] we could identify no autocrine interactions in the myeloblast population involving CCL3, CCL5, CXCL1, CXCL2, or CXCL8 (supplemental Figure 2C). These data support a model in which the BM microenvironment provides a protective sanctuary from gilteritinib in unresponsive patients via paracrine signaling from the myeloblasts.

Per-cell expression of FLT3 was also noted to increase post-treatment in unresponsive patients (Figure 2D). Samples from a gilteritinib-sensitive and -unresponsive patient pre-treatment at approximately cycle 1 day 30 were analyzed (supplemental Table 2) for FLT3/CD135 and pSTAT5 expression via spectral flow (Figure 3; supplemental Figure 3). In the sensitive sample, there was a decrease in the MFI for both FLT3 and pSTAT5 (Figure 3A). Furthermore, when specifically looking at the pSTAT5 scatter plot in the pre-treatment sample, there were two positive populations, of which the brightest population decreased post-treatment. For the unresponsive sample, there was an increase in MFI for FLT3

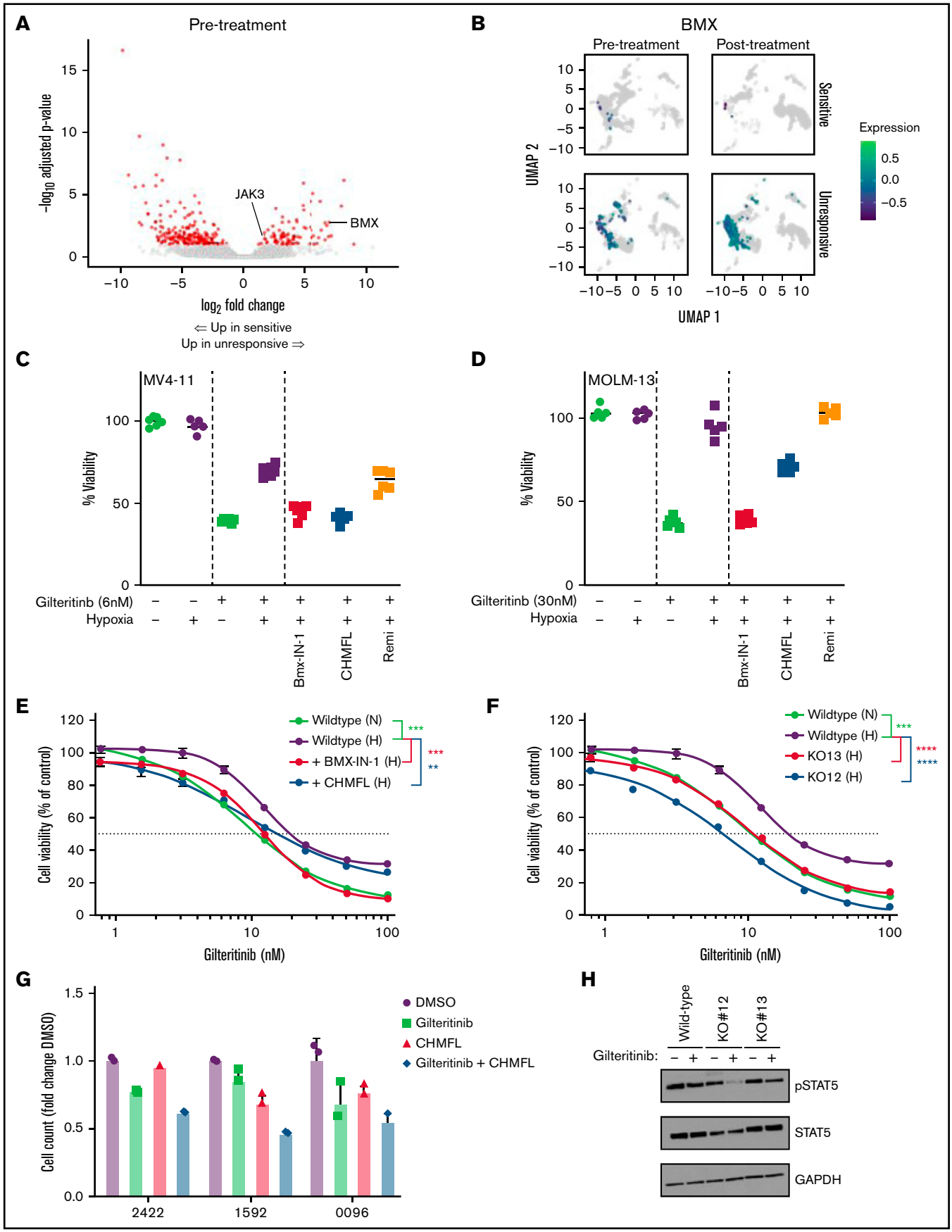
A
Pre-treatment
−log10 adjusted p-value
log2 fold change
JAK3
BMX
⇐ Up in sensitive
Up in unresponsive ⇒
B
BMX
Pre-treatment
Post-treatment
Sensitive
Unresponsive
UMAP 2
UMAP 1
Expression
C
MV4-11
% Viability
Gilteritinb (6nM)
Hypoxia
Bmx-IN-1
CHMFL
Remi
D
MOLM-13
% Viability
Gilteritinb (30nM)
Hypoxia
Bmx-IN-1
CHMFL
Remi
E
Wildtype (N)
Wildtype (H)
+ BMX-IN-1 (H)
+ CHMFL (H)
Cell viability (% of control)
Gilteritinib (nM)
F
Wildtype (N)
Wildtype (H)
KO13 (H)
KO12 (H)
Cell viability (% of control)
Gilteritinib (nM)
G
DMSO
Gilteritinib
CHMFL
Gilteritinib + CHMFL
Cell count (fold change DMSO)
2422
1592
0096
H
Wild-type
KO#12
KO#13
Gilteritinib:
pSTAT5
STAT5
GAPDH

Figure 4.

(Figure 3B). We also observed marginal changes in pSTAT5 (Figure 3B). These spectral flow data support our scRNASeq observations that there are differences in FLT3 signaling/expression between the sensitive and unresponsive groups.

BMX kinase mediates gilteritinib resistance

In order to identify differentially regulated genes that may predispose myeloblasts to gilteritinib resistance, we examined the pseudobulk RNA-seq signatures at pre-treatment. We observed higher gene expression for *BMX* and *JAK3* (Log_2-fold change, 6.65 and 1.72; adjusted *P* values, 0.00186 and 0.0391, respectively; Figure 4A; supplemental Table 5). BMX is a Tec kinase that has been associated with sorafenib resistance in *FLT3*+ AML through a STAT5-dependent compensatory signaling mechanism.[30] JAK3 is also able to signal independently of FLT3 through STAT5.[31] Given the important role that BMX plays in sorafenib resistance through activation of pro-survival signaling pathways in *FLT3*-ITD+ AML, we wanted to further explore a possible role for BMX in mediating gilteritinib resistance. *BMX* expression was strongly upregulated in unresponsive pre-treatment samples compared with the sensitive pre-treatment samples; BMX expression increased further post-treatment in unresponsive patients (Figure 4B). Furthermore, even though the relative levels of *BMX* expression in the sensitive group were low initially, a decrease in *BMX* expression was observed in the post-treatment myeloblasts (Figure 4B).

To decipher the functional role of BMX in mediating gilteritinib resistance, we cultured *FLT3*+ cell lines, MV4-11 and MOLM-13 in hypoxia, which activates BMX (supplemental Figure 4A),[30] and analyzed the response to gilteritinib. Reduced sensitivity to gilteritinib under hypoxic conditions compared with normoxia was observed (Figure 4C-D). We then pharmacologically inhibited BMX to determine if treatment could restore gilteritinib sensitivity in hypoxia. BMX-IN-1 and CHMFL-BMX-078 were used as selective inhibitors for BMX, determined by KdElect and a Kinase assay[32,33] (supplemental Tables 8-9). Remibrutinib, a selective BTK inhibitor, was used as control[34] (supplemental Table 8). BMX-IN-1 has been reported to dephosphorylate and degrade BMX, whereas CHMFL-BMX-078 results in dephosphorylation of BMX, but not degradation.[32,33] We observed similar results when MV4-11 and MOLM-13 cells were treated with BMX-IN-1 and CHMFL-BMX-078 (supplemental Figure 4B). Inhibitor concentrations were selected that had minimal effects on viability but inhibited BMX, as determined by western blot (supplemental Figure 4B-C). When combined with gilteritinib at a single concentration, treatment with selective BMX inhibitors restored gilteritinib sensitivity under hypoxic conditions; conversely, no change in gilteritinib resistance was observed when treated with remibrutinib under hypoxic conditions (Figure 4C-D). We then used MV4-11 cells to look for changes in gilteritinib IC_{50} when treated with BMX inhibitors under hypoxic conditions. Reversal in gilteritinib resistance was also observed after treatment with BMX-IN-1 or CHMFL-BMX-078, with a shift in IC_{50} from 19.2 to 12.3 or 15.2 nM, respectively (Figure 4E). To further verify the functional role BMX plays in mediating gilteritinib resistance, a BMX CRISPR KO line was generated from MV4-11 cells (supplemental Figure 4D-E). Two BMX CRISPR KO clones were carried forward for analysis to account for potential off-target effects. IC_{50} analysis showed a shift in gilteritinib sensitivity for both BMX KO clones (6.7 and 11.4 nM) compared with wild-type MV4-11 cells (19.5 nM) under activating hypoxic conditions (Figure 4F).

Next, we wanted to test whether pharmacological inhibition of BMX by CHMFL-BMX-078 in primary *FLT3*+ AML samples ex vivo altered gilteritinib sensitivity under hypoxic conditions. Using primary *FLT3*+ AML samples, with common co-occurring mutations (supplemental Table 10) and expressing BMX (supplemental Figure 4F), we found CHMFL-BMX-078 sensitized cells to gilteritinib (Figure 4G; supplemental Figure 4G). Additionally, the combination of gilteritinib and CHMFL-BMX-078 was additive-to-synergistic in these primary AML samples (supplemental Figure 4H).

To understand the mechanism responsible for BMX-mediated gilteritinib resistance, we examined pSTAT5 signaling in the MV4-11 wild-type and BMX KO clones. Previously, BMX was shown to provide a STAT5-dependent compensatory signaling mechanism in *FLT3*-ITD+ cell lines in response to sorafenib treatment.[30] We found that under BMX-activating conditions, pSTAT5 signaling decreased minimally in the wild-type MV4-11 cells after gilteritinib treatment. However, under the same culturing conditions, the BMX KO clones showed a greater decrease in pSTAT5 signaling (Figure 4H; supplemental Figure 4I).

These data suggest that BMX alters STAT5 signaling and supports the notion that BMX contributes to gilteritinib resistance in a hypoxia-dependent manner, as well as may help to explain the lack of response in primary patient samples with high baseline expression of BMX. Furthermore, inhibition of BMX, with an inhibitor like CHMFL-BMX-078, can increase antileukemic activity of gilteritinib in *FLT3*+ primary samples with high BMX baseline expression.

Figure 4 (continued) BMX kinase mediates resistance to gilteritinib. (A) Differential gene expression for gilteritinib-unresponsive patients. Red indicates genes with adjusted $P < .1$ and fold change ≥1.5; see also supplemental Table 5. (B) UMAP representation of myeloblast cells stratified by gilteritinib response (rows) and time point relative to starting therapy (columns). BMX expression is shown as the Log_{10}-transformed and color scheme corresponds to scale shown. (C) MV4-11 and (D) MOLM-13 grown under normoxic (−) or hypoxic (+) conditions for 24 hours, followed by treatment with gilteritinib (+) alone or in combination with BMX-IN-1 (1.5 and 2.5 μM, respectively), CHMFL-BMX-078 (3 and 5 μM, respectively) or remibrutinib (3 and 5 μM, respectively) for 48 hours. Cell viability was assessed by MTT (n = 4-6). Representative data of three independent experiments. (E) MV4-11 was cultured in hypoxia (H) or normoxia (N) for 24 hours. Inhibition by gilteritinib alone or in combination with BMX-IN-1 (1.5 μM) or CHMFL-BMX-078 (3 μM) was determined after 48 hours by MTT (n = 6). Representative data of two independent experiments. (F) MV4-11 wild-type and BMX CRISPR KO was cultured in hypoxia (H) or normoxia (N) for 24 hours, treated with increasing concentration of gilteritinib for 48 hours and assessed by MTT (n = 6). Representative data of two independent experiments. (G) Inhibition of cell growth of human primary *FLT3*-mutated AML samples treated with gilteritinib (100 nM) alone, CHMFL-BMX-078 (1.5 μM) alone, or the combination. Samples were grown in hypoxia for 24 hours, treated for 48 hours, and viability was determined by CellTiter-Glo assay (n = 3). (H) MV4-11 wild-type and BMX CRISPR knockout cells were cultured in hypoxia for 24 hours and treated with 5 nM gilteritinib for 1 hour. Western blots were carried. Representative data from three independent experiments shown. For statistical analysis, $^{**}P \leq .01$, $^{***}P \leq .001$, $^{****}P \leq .0001$, as determined by two-tailed, unpaired Student *t* test.

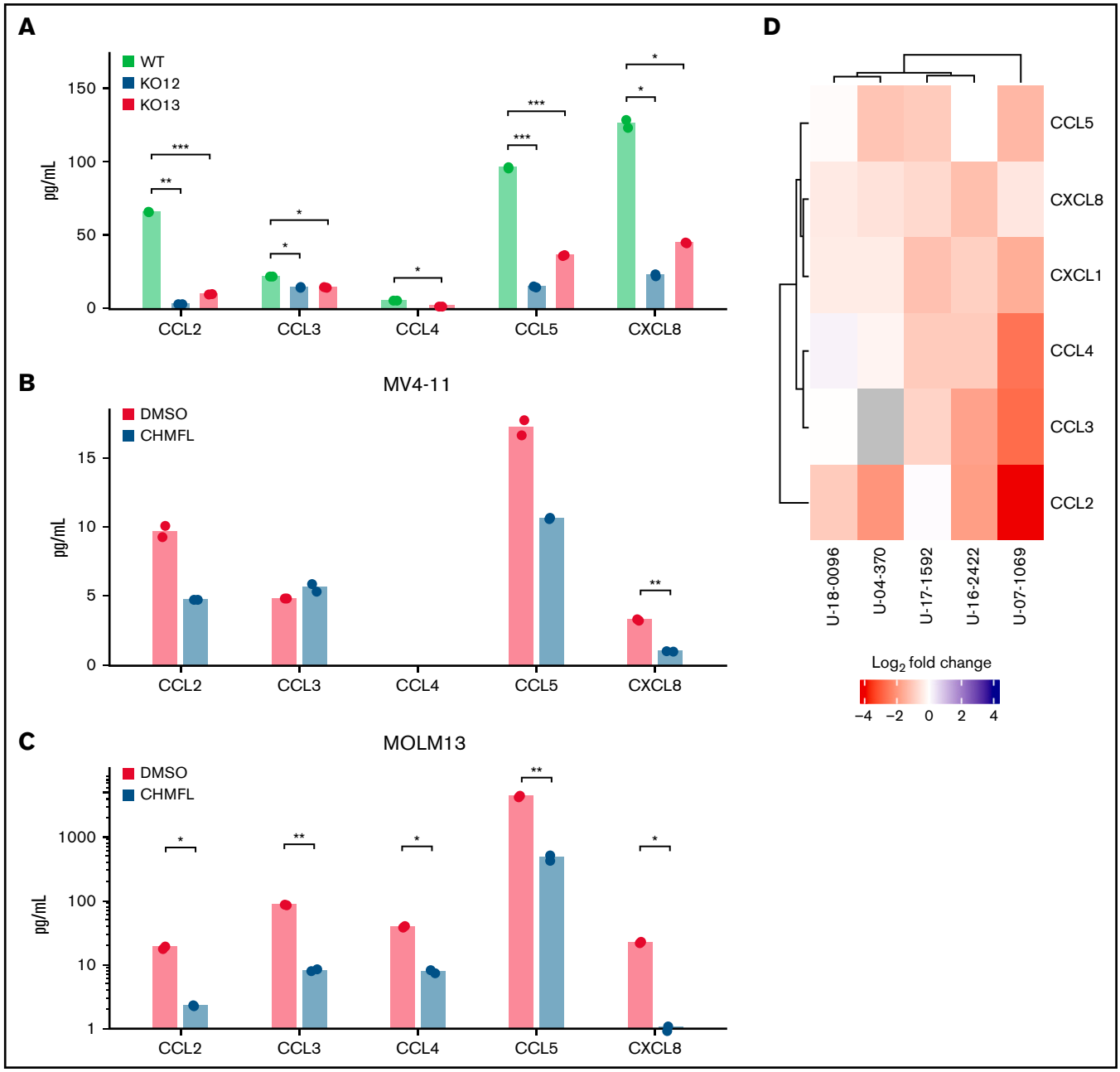

Figure 5. Cytokine/chemokine secretion in response to BMX inhibition or knockout. (A) Cytokines/chemokines secreted by MV4-11 wild-type and BMX CRISPR KO cells, after 72 hours in hypoxia (Luminex multiplex assay, n = 2). Representative data from two independent experiments are shown. Cytokines/chemokines secreted by (B) MV4-11 and (C) MOLM-13, after growth in hypoxic conditions for 24 hours, followed by treatment with CHMFL-BMX-078 (3 and 5 μM, respectively) for 48 hours (Luminex multiplex assay, n = 2). Representative data from two independent experiments shown. (D) Secretion of cytokines/chemokines by human primary *FLT3*+ AML samples cultured in hypoxia for 24 hours, followed by treatment with CHMFL-BMX-078 for 48 hours (Luminex multiplex assay, n = 2). For statistical analysis, *$P \leq .05$; **$P \leq .01$; ***$P \leq .001$, as determined by two-tailed, unpaired Student *t* test.

BMX alters the cytokine/chemokine network

Although the signal transduction pathways involving BMX are poorly characterized, various investigations suggest that BMX can signal downstream from multiple growth factor and cell surface receptors.[35] We wanted to determine if BMX could modulate cytokine/chemokine secretion under activating conditions. We focused on the AML CCL2-4/CXCL1/8 chemokine/cytokine cluster whose levels are known to increase with exposure to hypoxia[36] and CCL5, which was upregulated in the pseudobulk RNA-seq analysis. When comparing the secretion of these chemokines between MV4-11 wild-type and BMX CRISPR KO clones in hypoxic conditions, both KO clones were found to have lower secretion compared with wild type (Figure 5A). When BMX was pharmacologically inhibited by CHMFL-BMX-078, secretion of these chemokines was also

decreased in both MV4-11 and MOLM-13 under hypoxic conditions (Figure 5B-C). Furthermore, when we treated primary *FLT3*+ AML samples with CHMFL-BMX-078 in hypoxia, we also observed a downregulation of these chemokines (Figure 5D; supplemental Table 11). These results support a novel role for BMX in modulating the cytokine/chemokine network with AML cells in the hypoxic microenvironment.

Discussion

Lack of response or relapse after initial response to a FLT3 inhibitor remains an issue in *FLT3*+ AML. Deciphering these molecular mechanisms involved in resistance is essential to improving treatment strategies and outcomes. Here we show that BMX expression is higher in gilteritinib-unresponsive patients prior to treatment, possibly related to a hypoxic state in the marrow microenvironment, and that BMX expression is essential for chemokine and cytokine production by AML cells under hypoxic conditions. BMX activation in the AML cells potentiates a set of signaling pathways leading to production of cytokines and chemokines after initiation of gilteritinib, which then act on the marrow microenvironment in a paracrine fashion. In addition, upregulation of BMX expression can bypass FLT3 and directly activate STAT5, a pro-survival signal for the maintenance and expansion of AML blasts.[37,38] BMX has previously been shown to signal through STAT5 independently of FLT3.[30,39,40] Indeed, we observed sensitization to gilteritinib treatment in hypoxic conditions when BMX was either knocked out or pharmacologically inhibited, which was associated with a reduction in STAT5 phosphorylation. Thus, BMX activation bypasses FLT3 inhibition by gilteritinib and can act as a resistance pathway in AML.

In gilteritinib-unresponsive patient samples, upregulation of BMX expression was associated with an increase in BM-derived cytokine/chemokine expression that was not observed in gilteritinib-sensitive patient samples. BM microenvironmental factors have been shown to protect *FLT3*+ AML from FLT3 inhibitors,[25-28,41] other studies have shown that AML utilizes these factors to promote disease progression and relapse.[42,43] In AML, CCL2-4/CXCL1/8 cluster reshapes the microenvironment through bidirectional interactions within BM niche cells: CCL2/CCR2 have been implicated in the activation of intracellular pathways connected with survival, proliferation, and growth, as well as the suppression of the infiltration of tumor-associated macrophages.[44,45] CXCL8 and its receptors CXCR1/CXCR2 are involved in bidirectional cross talk between the primary AML cells and the microenvironment, but also contribute to leukemia progression through an autocrine loop.[43] CCL3 signaling is involved in leukemogenesis[46] and remodeling of the microenvironment to further support leukemic cell growth.[43] In our study, the myeloblast population showed low levels of expression of the receptors for these microenvironmental factors, arguing against autocrine action and suggesting the presence of paracrine effects on the microenvironment supporting gilteritinib resistance.

Here we demonstrated a novel, functional link between BMX and its ability to modulate the cytokine/chemokine network: genetic or chemical interruption of BMX signaling reduced chemokine production by AML cell lines and primary cells under hypoxic conditions. The ENCODE transcription factor target database predicts CXCL2, CCL3, CCL4, and CCL5 as potential targets of STAT5, linking BMX and STAT5 activation to the cytokine/chemokine network. CXCL8 is primarily activated by NF-kB, which in turn can be activated by BMX.[47,48] The ability of BMX inhibition to reduce the secretion profile of these chemokine/cytokines by AML cells suggests the potential benefit of pursuing BMX as a therapeutic target. For example, *FLT3*+ AML patients with high BMX expression could benefit from the addition of TL-895, a leading clinical BMX inhibitor candidate, to gilteritinib. Thus, an improved understanding of the molecular mechanisms of gilteritinib resistance may allow for the advancement of rational combination of therapies that could improve the poor prognosis of patients with *FLT3*+ AML.

Acknowledgments

The authors thank the following Ohio State University Comprehensive Cancer Center (OSUCCC) Shared Resources: Genomics Shared Resource, Flow Cytometry Shared Resource, and the LTBSR for access to primary AML patient samples.

This work was supported by National Institutes of Health grants P30 CA021765, R01 CA138744 (to S.D.B.) and R01 DK128238 (to B.W.B.), the Ohio State University Comprehensive Cancer Center Pelotonia Foundation (to S.D.B. and B.W.B.), and the National Center for Advancing Translational Sciences UL1TR002733 Award.

The content is solely the responsibility of the authors and does not represent the official views of the funding agencies.

Authorship

Contribution: D.R.B. conceptualization, data curation, formal analysis, investigation, methodology, validation, visualization, writing–original draft, writing–review and editing; B.B. investigation, formal analysis; S.J.O. data curation, investigation, formal analysis, validation, visualization; J.Y.J. investigation, formal analysis; E.D.E. investigation; J.C.S. investigation; N.P conceptualization, data curation, formal analysis, investigation, writing–review and editing; J.S.B. conceptualization, methodology; S.D.B. conceptualization, funding acquisition, project administration, supervision, writing–review and editing; B.W.B. conceptualization, funding acquisition, project administration, supervision, writing–review and editing; and all authors read and approved the final manuscript.

Conflict-of-interest disclosure: The authors declare no potential conflicts of interest.

ORCID profiles: D.R.B., 0000-0002-4413-5711; B.B., 0000-0002-4869-0712; S.J.O., 0000-0002-4537-1409; E.D.E., 0000-0003-1176-675X; N.S.P., 0000-0001-9408-0539; J.S.B., 0000-0002-4275-5562; S.D.B., 0000-0003-3062-3252; B.W.B., 0000-0002-3168-5423.

Correspondence: Bradley W. Blaser, 400W 12th Ave, 302A Wiseman Hall, Columbus, OH 43210; e-mail: bradley.blaser@osumc.edu; and Sharyn D. Baker, 460 W 12th Ave, 410 Biomedical Research Tower, Columbus, OH 43210; e-mail: baker.2480@osu.edu.

References

1. Ley TJ, Miller C, Ding L, et al; Cancer Genome Atlas Research Network. Genomic and epigenomic landscapes of adult de novo acute myeloid leukemia. *N Engl J Med.* 2013;368(22):2059-2074.
2. Papaemmanuil E, Gerstung M, Bullinger L, et al. Genomic classification and prognosis in acute myeloid leukemia. *N Engl J Med.* 2016;374(23):2209-2221.
3. Patel JP, Gönen M, Figueroa ME, et al. Prognostic relevance of integrated genetic profiling in acute myeloid leukemia. *N Engl J Med.* 2012;366(12):1079-1089.
4. Thiede C, Steudel C, Mohr B, et al. Analysis of FLT3-activating mutations in 979 patients with acute myelogenous leukemia: association with FAB subtypes and identification of subgroups with poor prognosis. *Blood.* 2002;99(12):4326-4335.
5. Meshinchi S, Woods WG, Stirewalt DL, et al. Prevalence and prognostic significance of Flt3 internal tandem duplication in pediatric acute myeloid leukemia. *Blood.* 2001;97(1):89-94.
6. Wu X, Feng X, Zhao X, et al. Prognostic significance of FLT3-ITD in pediatric acute myeloid leukemia: a meta-analysis of cohort studies. *Mol Cell Biochem.* 2016;420(1-2):121-128.
7. Zwaan CM, Meshinchi S, Radich JP, et al. FLT3 internal tandem duplication in 234 children with acute myeloid leukemia: prognostic significance and relation to cellular drug resistance. *Blood.* 2003;102(7):2387-2394.
8. Levis M. Midostaurin approved for FLT3-mutated AML. *Blood.* 2017;129(26):3403-3406.
9. Perl AE, Martinelli G, Cortes JE, et al. Gilteritinib or chemotherapy for relapsed or refractory *FLT3*-mutated AML. *N Engl J Med.* 2019;381(18):1728-1740.
10. Eguchi M, Minami Y, Kuzume A, Chi S. Mechanisms underlying resistance to FLT3 inhibitors in acute myeloid leukemia. *Biomedicines.* 2020;8(8):245.
11. McMahon CM, Ferng T, Canaani J, et al. Clonal selection with RAS pathway activation mediates secondary clinical resistance to selective FLT3 Inhibition in acute myeloid leukemia. *Cancer Discov.* 2019;9(8):1050-1063.
12. Joshi SK, Nechiporuk T, Bottomly D, et al. The AML microenvironment catalyzes a stepwise evolution to gilteritinib resistance. *Cancer Cell.* 2021;39(7):999-1014.e8.
13. Zavorka Thomas ME, Lu X, Talebi Z, et al. Gilteritinib inhibits glutamine uptake and utilization in *FLT3*-ITD-positive AML. *Mol Cancer Ther.* 2021;20(11):2207-2217.
14. Eisfeld AK, Kohlschmidt J, Mrózek K, et al. Adult acute myeloid leukemia with trisomy 11 as the sole abnormality is characterized by the presence of five distinct gene mutations: MLL-PTD, DNMT3A, U2AF1, FLT3-ITD and IDH2. *Leukemia.* 2016;30(11):2254-2258.
15. McCarthy DJ, Campbell KR, Lun AT, Wills QF. Scater: pre-processing, quality control, normalization and visualization of single-cell RNA-seq data in R. *Bioinformatics.* 2017;33(8):1179-1186.
16. McGinnis CS, Murrow LM, Gartner ZJ. DoubletFinder: doublet detection in single-cell RNA sequencing data using artificial nearest neighbors. *Cell Syst.* 2019;8(4):329-337.e4.
17. Haghverdi L, Lun ATL, Morgan MD, Marioni JC. Batch effects in single-cell RNA-sequencing data are corrected by matching mutual nearest neighbors. *Nat Biotechnol.* 2018;36(5):421-427.
18. Trapnell C, Cacchiarelli D, Grimsby J, et al. The dynamics and regulators of cell fate decisions are revealed by pseudotemporal ordering of single cells. *Nat Biotechnol.* 2014;32(4):381-386.
19. Cao J, Spielmann M, Qiu X, et al. The single-cell transcriptional landscape of mammalian organogenesis [published correction appears in https://doi.org/10.17504/protocols.io.9yih7ue]. *Nature.* 2019;566(7745):496-502.
20. Wolf FA, Hamey FK, Plass M, et al. PAGA: graph abstraction reconciles clustering with trajectory inference through a topology preserving map of single cells. *Genome Biol.* 2019;20(1):59.
21. Hao Y, Hao S, Andersen-Nissen E, et al. Integrated analysis of multimodal single-cell data. *Cell.* 2021;184(13):3573-3587.e29.
22. Love MI, Huber W, Anders S. Moderated estimation of fold change and dispersion for RNA-seq data with DESeq2. *Genome Biol.* 2014;15(12):550.
23. Jin S, Guerrero-Juarez CF, Zhang L, et al. Inference and analysis of cell-cell communication using CellChat. *Nat Commun.* 2021;12(1):1088.
24. Di Veroli GY, Fornari C, Wang D, et al. Combenefit: an interactive platform for the analysis and visualization of drug combinations. *Bioinformatics.* 2016;32(18):2866-2868.
25. Yang X, Sexauer A, Levis M. Bone marrow stroma-mediated resistance to FLT3 inhibitors in FLT3-ITD AML is mediated by persistent activation of extracellular regulated kinase. *Br J Haematol.* 2013;164(1):61-72.
26. Traer E, Martinez J, Javidi-Sharifi N, et al. FGF2 from marrow microenvironment promotes resistance to FLT3 inhibitors in acute myeloid leukemia. *Cancer Res.* 2016;76(22):6471-6482.
27. Sung PJ, Sugita M, Koblish H, Perl AE, Carroll M. Hematopoietic cytokines mediate resistance to targeted therapy in FLT3-ITD acute myeloid leukemia. *Blood Adv.* 2019;3(7):1061-1072.
28. Dumas PY, Naudin C, Martin-Lannerée S, et al. Hematopoietic niche drives FLT3-ITD acute myeloid leukemia resistance to quizartinib *via* STAT5-and hypoxia-dependent upregulation of AXL. *Haematologica.* 2019;104(10):2017-2027.

29. Jeon JY, Buelow DR, Garrison DA, et al. TP-0903 is active in models of drug-resistant acute myeloid leukemia. *JCI Insight.* 2020;5(23):140169.

30. van Oosterwijk JG, Buelow DR, Drenberg CD, et al. Hypoxia-induced upregulation of BMX kinase mediates therapeutic resistance in acute myeloid leukemia. *J Clin Invest.* 2017;128(1):369-380.

31. Baker SJ, Rane SG, Reddy EP. Hematopoietic cytokine receptor signaling. *Oncogene.* 2007;26(47):6724-6737.

32. Liu F, Zhang X, Weisberg E, et al. Discovery of a selective irreversible BMX inhibitor for prostate cancer. *ACS Chem Biol.* 2013;8(7):1423-1428.

33. Liang X, Lv F, Wang B, et al. Discovery of 2-((3-Acrylamido-4-methylphenyl)amino)-*N*-(2-methyl-5-(3,4,5-trimethoxybenzamido)p henyl)-4-(methylamino)pyrimidine-5-carboxamide (CHMFL-BMX-078) as a highly potent and selective type II irreversible bone marrow kinase in the X chromosome (BMX) kinase inhibitor. *J Med Chem.* 2017;60(5):1793-1816.

34. Angst D, Gessier F, Janser P, et al. Discovery of LOU064 (Remibrutinib), a potent and highly selective covalent inhibitor of Bruton's tyrosine kinase. *J Med Chem.* 2020;63(10):5102-5118.

35. Seixas JD, Sousa BB, Marques MC, et al. Structural and biophysical insights into the mode of covalent binding of rationally designed potent BMX inhibitors. *RSC Chem Biol.* 2020;1(4):251-262.

36. Kittang AO, Hatfield K, Sand K, Reikvam H, Bruserud Ø. The chemokine network in acute myelogenous leukemia: molecular mechanisms involved in leukemogenesis and therapeutic implications. *Curr Top Microbiol Immunol.* 2010;341:149-172.

37. Carroll M, Kim TK, Higashino K, Gewirtz AM. Acute myeloid leukemia cells require STAT5 for survival. *Blood.* 2005;106(11):1616.

38. Schepers H, van Gosliga D, Wierenga AT, Eggen BJ, Schuringa JJ, Vellenga E. STAT5 is required for long-term maintenance of normal and leukemic human stem/progenitor cells. *Blood.* 2007;110(8):2880-2888.

39. Saharinen P, Ekman N, Sarvas K, Parker P, Alitalo K, Silvennoinen O. The BMX tyrosine kinase induces activation of the Stat signaling pathway, which is specifically inhibited by protein kinase Cδ. *Blood.* 1997;90(11):4341-4353.

40. Guryanova OA, Wu Q, Cheng L, et al. Nonreceptor tyrosine kinase BMX maintains self-renewal and tumorigenic potential of glioblastoma stem cells by activating STAT3. *Cancer Cell.* 2011;19(4):498-511.

41. Beeharry N, Landrette S, Gayle S, et al. LAM-003, a new drug for treatment of tyrosine kinase inhibitor-resistant FLT3-ITD-positive AML. *Blood Adv.* 2019;3(22):3661-3673.

42. Binder S, Luciano M, Horejs-Hoeck J. The cytokine network in acute myeloid leukemia (AML): a focus on pro- and anti-inflammatory mediators. *Cytokine Growth Factor Rev.* 2018;43:8-15.

43. Pievani A, Biondi M, Tomasoni C, Biondi A, Serafini M. Location first: targeting acute myeloid leukemia within its niche. *J Clin Med.* 2020;9(5):1513.

44. Melgarejo E, Medina MA, Sánchez-Jiménez F, Urdiales JL. Monocyte chemoattractant protein-1: a key mediator in inflammatory processes. *Int J Biochem Cell Biol.* 2009;41(5):998-1001.

45. Fei L, Ren X, Yu H, Zhan Y. Targeting the CCL2/CCR2 axis in cancer immunotherapy: one stone, three birds? *Front Immunol.* 2021;12:771210.

46. Staversky RJ, Georger MA, Ackun-Farmmer M, et al. CCL3 signaling is essential for leukemia progression but dispensable for hematopoietic stem cell maintenance. *Blood.* 2017;130(suppl 1):2603.

47. Gottar-Guillier M, Dodeller F, Huesken D, et al. The tyrosine kinase BMX is an essential mediator of inflammatory arthritis in a kinase-independent manner. *J Immunol.* 2011;186(10):6014-6023.

48. Ha H, Debnath B, Neamati N. Role of the CXCL8-CXCR1/2 axis in cancer and inflammatory diseases. *Theranostics.* 2017;7(6):1543-1588.